Electrochemistry Communications 58 (2015) 51–56

Contents lists available at ScienceDirect

Electrochemistry Communications

journal homepage: www.elsevier.com/locate/elecom

Short communication

Porphyrin-based metal–organic framework thin films for electrochemical nitrite detection

Chung-Wei Kung [a], Ting-Hsiang Chang [a], Li-Yao Chou [a], Joseph T. Hupp [b], Omar K. Farha [b,c], Kuo-Chuan Ho [a,d,*]

[a] Department of Chemical Engineering, National Taiwan University, Taipei 10617, Taiwan
[b] Department of Chemistry, Northwestern University, Evanston, IL 60208, United States
[c] Department of Chemistry, Faculty of Science, King Abdulaziz University, Jeddah, Saudi
[d] Institute of Polymer Science and Engineering, National Taiwan University, Taipei 10617, Taiwan

ARTICLE INFO

Article history:
Received 11 May 2015
Received in revised form 3 June 2015
Accepted 6 June 2015
Available online 14 June 2015

Keywords:
Electroactive metal–organic frameworks
Electrocatalysis
Electrochemical sensor
Solvothermal growth
Zirconium node

ABSTRACT

Uniform zirconium-based porphyrin metal–organic framework (MOF-525) thin films are grown on conducting glass substrates by using a solvothermal approach. The obtained MOF-525 thin film is electrochemically addressable in aqueous solution and shows electrocatalytic activity for nitrite oxidation. The mechanism for the electrocatalytic oxidation of nitrite at the MOF-525 thin film is investigated by cyclic voltammetry. The redox mechanism of the MOF-525 thin film in the KCl aqueous solution is studied by amperometry. The MOF-525 thin film is deployed as an amperometric nitrite sensor. The linear range, sensitivity, and limit of detection are 20–800 μM, 95 μA/mM-cm^2, and 2.1 μM, respectively.

1. Introduction

Nitrite has been widely used as a preserving agent and appearance builder in the food industry. However, excess uptake of nitrite is harmful to human health [1,2]. Furthermore, it is well known that the appearance of nitrite in human urine is often correlated with urinary tract infections [3]. Thus, accurate detection of nitrite becomes an important issue in both the food and health industries.

Several analytical techniques have been developed for detecting nitrite [4–7]. Compared to other approaches, electrochemical detection shows the advantages of simple experimental procedures, short response time, and feasibility for building portable sensors [8]. Therefore, various materials have been utilized as electrocatalytic materials for detecting nitrite electrochemically [9–14]. In addition to these materials, porphyrins and metalloporphyrins have been reported as electrocatalysts for the oxidation of nitrite [15–17]. To further improve the sensitivity of the electrochemical sensor, more electrocatalytic sites are required on the modified electrode.

Metal–organic frameworks (MOFs) are a series of porous materials which are constructed with metal-based nodes and organic linkers [18,19]. Due to their regular porosity and tunable pore compositions, MOFs have been examined for various applications [20–27]. The highest Brunauer–Emmett–Teller (BET) surface area of MOFs reported in the literature exceeds 7000 m^2/g, which is much higher than the values of other porous materials [28]. Due to such high surface area, a few studies have utilized MOFs for electrochemical sensors [29–32]. Among various MOFs, porphyrin MOFs, which are constructed from porphyrinic or metalloporphyrinic linkers, have been widely reported [33–35]. The thin films of porphyrin MOFs grown on substrates have also been reported [36–39], however, only a few studies report their electrochemistry and electrochemical applications [38]. Given the high surface areas of MOFs, we reasoned that a water-stable porphyrin MOF thin film grown on a conducting substrate should be an attractive candidate for electrochemical nitrite sensor. To date there is not any study utilizing porphyrin MOFs for electrochemical detection of nitrite.

Recently, we prepared uniformly grown porphyrin MOF thin films on conducting glass substrates solvothermally; the MOF is constructed from free-base meso-tetra(4-carboxyphenyl)porphine (H_4TCPP) linkers and hexa-zirconium nodes (MOF-525; Fig. 1(a)) [40]. The MOF-525 sample possessed a BET surface area of 2415 m^2/g, with a unique pore size of 1.8 nm. Moreover, the MOF-525 thin film was found to be electrochemically addressable and stable in aqueous solution [40]. However, applications of the MOF-525 thin film have not

* Corresponding author at: Department of Chemical Engineering, National Taiwan University, Taipei 10617, Taiwan. Tel.: +886 2 2366 0739; fax: +886 2 2362 3040.
E-mail address: kcho@ntu.edu.tw (K.-C. Ho).

http://dx.doi.org/10.1016/j.elecom.2015.06.003
1388-2481/

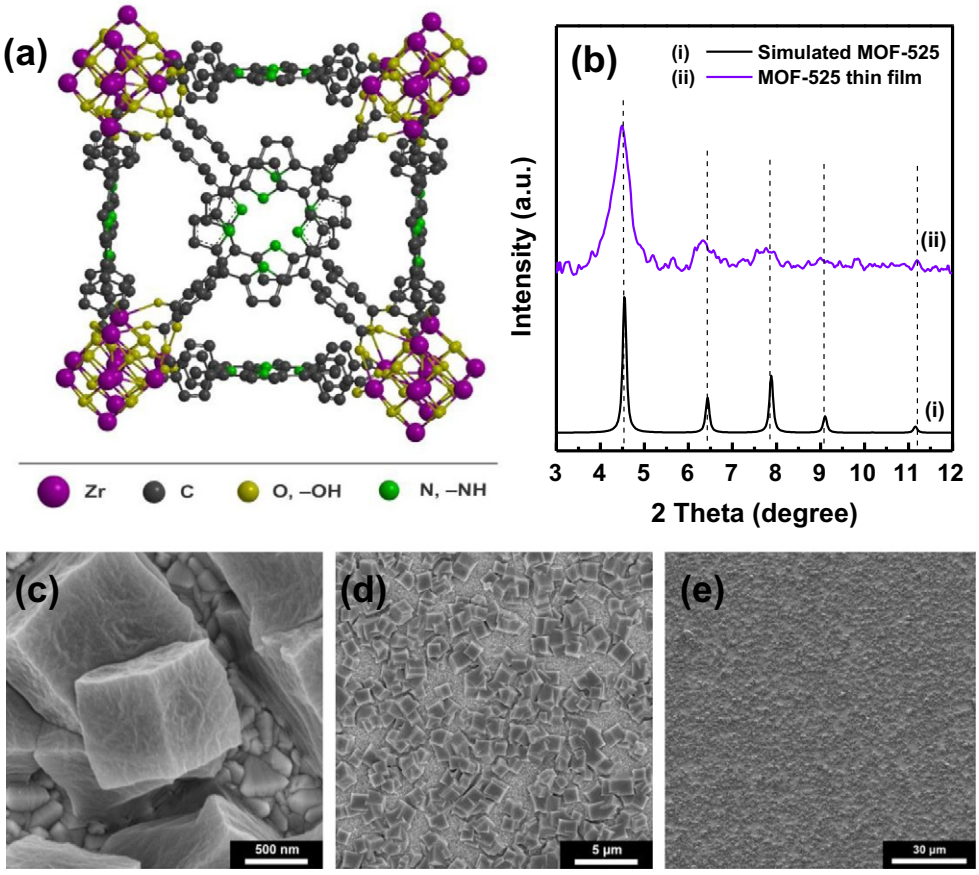

Fig. 1. (a) Crystal structure of MOF-525. For simplicity hydrogen atoms are omitted. (b) XRD patterns of the MOF-525 thin film and simulated MOF-525 [35]. (c)–(e) SEM images of the MOF-525 thin film at various magnifications.

been explored. Due to the ultrahigh stability of zirconium-based MOFs in water [41], the electroactive MOF-525 thin film seems to be appropriate for electrochemical sensing applications in aqueous systems.

2. Material and methods

Potassium chloride (Sigma-Aldrich, 99.0–100.5%), and sodium nitrite ($NaNO_2$, Sigma-Aldrich, ≥99.0%) were used as received. Deionized water was used throughout the work. The experimental procedure for the growth of MOF-525 thin film has been reported in details in our previous study [40]; uniform MOF-525 thin films with dark red color can be grown on fluorine-doped tin oxide (FTO) substrates with excellent reproducibility. The hydroxyl groups covering on the FTO substrate are necessary for the growth of MOF thin film with strong chemical bonding to the substrate [26,27,38,40].

X-ray diffraction (XRD) patterns were measured by an X-ray diffractometer (X-Pert, the Netherlands). The morphologies of MOF-525 thin films were investigated by a scanning electron microscope (SEM, Nova NanoSEM 230). All the electrochemical measurements were conducted on a CHI 440 electrochemical workstation (CH Instruments, Inc., USA), using a three-electrode setup. The MOF-525 thin film or bare FTO glass (0.25 cm^2) was served as the working electrode. A Pt foil (4 cm^2) and a Ag/AgCl/KCl (sat'd) electrode (homemade) were served as the counter and reference electrodes, respectively. 10 mL of 0.1 M KCl aqueous solution was used as the electrolyte.

3. Results and discussion

3.1. Characterizations

Fig. 1(b) shows the XRD pattern of the obtained MOF-525 thin film and the simulated XRD pattern of MOF-525 reported by Morris *et al.* [35]. All the diffraction peaks observed in the experiment agree with the simulated pattern. Fig. 1(c) to (e) show the SEM images of the MOF-525 thin film at various magnifications. It can be observed that the thin film is composed of several cubic crystals of MOF-525 grown on the FTO surface, and it shows a uniform morphology over a large-area region (Fig. 1(e)).

3.2. Redox mechanism and electrocatalysis

Fig. 2(a) shows the cyclic voltammetric (CV) curves of the MOF-525 thin film and bare FTO substrate measured in 0.1 M KCl solutions before and after adding 0.5 mM of $NaNO_2$. For the bare FTO substrate, the current signal for the oxidation of nitrite is negligible. A broad redox hump can be observed in the CV curve of the MOF-525 thin film; this redox signal may be attributed to the oxidation of free-base TCPP linkers, which generates the cation radical state of the porphyrin ($TCPP^+$) [40,42]. Moreover, a remarkable current signal for the irreversible oxidation of nitrite (NO_2^-) can be observed in the CV curves of MOF-525 thin films. It should be noted that after immersing in 0.1 M $NaNO_2$ aqueous solution for 10 min and washing by DIW, the pretreated MOF-525 thin film shows a similar redox behavior, suggesting that the

chemisorption of nitrite inside the film is negligible. As reported previously, the oxidation process of nitrite happening on a platinum electrode involves the electrochemical oxidation of NO_2^- to NO_2 and the rapid disproportionation of NO_2 into NO_2^- and nitrate (NO_3^-) [43]. The chemical reaction between nitrite and protons does not contribute to any observable current since the electrochemistry was investigated in 0.1 M KCl solution, which shows a pH value much higher than the p*K*a of HNO_2 [44,45]. Accordingly, the whole electrocatalytic process happening at the MOF-525 thin film is proposed as follow:

$$2\text{TCPP} \leftrightarrow 2\text{TCPP}^+ + 2e^- \quad (1)$$

$$2\text{TCPP}^+ + 2NO_2^- \rightarrow 2NO_2 + 2\text{TCPP} \quad (2)$$

$$2NO_2 + H_2O \rightarrow NO_3^- + NO_2^- + 2H^+ \quad (3)$$

Fig. 2(b) shows CV curves of the MOF-525 thin film measured in 0.1 M KCl solutions containing various concentrations of nitrite. A broad anodic peak can be observed at around 0.85 V in all the CV curves after the addition of nitrite, and the peak current increases linearly with the increasing concentration of nitrite. The current increment of the MOF-525 thin film after adding nitrite is more than two orders of magnitude higher than that of the bare FTO substrate (Fig. 2(c)), which indicates the merit of using MOF-525 thin film as compared to the bare substrate.

Fig. 3(a) shows the CV curves of the MOF-525 thin film measured in 0.1 M KCl solution containing 1.0 mM of nitrite at various scan rates (ν). The values of anodic peak current density (J_{pa}) obtained from these CV curves are plotted *versus* ν and $\nu^{0.5}$, respectively (Fig. 3(b) and (c)). It can be observed that the value of J_{pa} exhibits excellent linearity with $\nu^{0.5}$ ($R^2 = 0.998$), which is much better than that with ν ($R^2 = 0.968$). This result indicates that the whole electrocatalytic process is diffusion-controlled [46]. In addition, a plot of $J_{pa}/\nu^{0.5}$ *versus* ν is shown in Fig. 3(d). The curve in Fig. 3(d) exhibits a shape typical of that for an ECcat process [47,48]; this result further supports the mechanism proposed in Eqs. (1)–(3).

To further investigate the redox mechanism of the MOF-525 thin film, amperometric method was utilized [49]. The MOF-525 thin film was first held at 0 V and immediately switched to 0.9 V at 0 s, and the plots of current density (J) *versus* $t^{-0.5}$ are shown in Fig. 3(e). From the slope of the plot, the diffusion coefficient (D) of the current-producing charges through the MOF-525 thin film can be estimated by using Cottrell equation [46,49–51]:

$$J = \frac{nFD^{0.5}C}{\pi^{0.5}} t^{-0.5} \quad (4)$$

where C is the concentration of redox active centers (*i.e.*, TCPP linkers) within the MOF-525 thin film, while n and F maintain their standard meanings. From the crystal structure of MOF-525, the value of C was estimated to be 681 mol/m^3. Thus, the value of D for oxidation-driven charge transport within the MOF-525 thin film in the 0.1 M KCl solution without nitrite was estimated to be 2.14×10^{-16} m^2/s. Since the physical movement of TCPP linkers in MOF-525 is negligible, the redox process of the MOF-525 thin film should be limited by either the charge hopping between the linkers or the diffusion of K^+ and/or Cl^- in the thin film [50,51].

The amperometric experiments were also performed in the presence of nitrite. As shown in Fig. 3(e), the slope increases with increasing nitrite concentration. The increases are expected for ECcat processes, as the observed current transients now contain contributions from simple charge-hopping as well as catalytic regeneration of the oxidizable form of the MOF linker. Given their dual origin, we will term the parameters derived from early-time Cottrell plots, *apparent* diffusion coefficients (D_{app}). The values of D_{app} were estimated to be 9.10×10^{-16}, 3.32×10^{-15}, and 6.30×10^{-15} m^2/s in the solutions containing 0.2, 0.4, and 0.6 mM of nitrite, respectively. In the presence of nitrite, nitrite ions coming from the bulk electrolyte can diffuse through the porous MOF thin film and get oxidized inside the film, which reduces the $TCPP^+$ back to TCPP (also see Eq. (2)). Under this situation, the charge

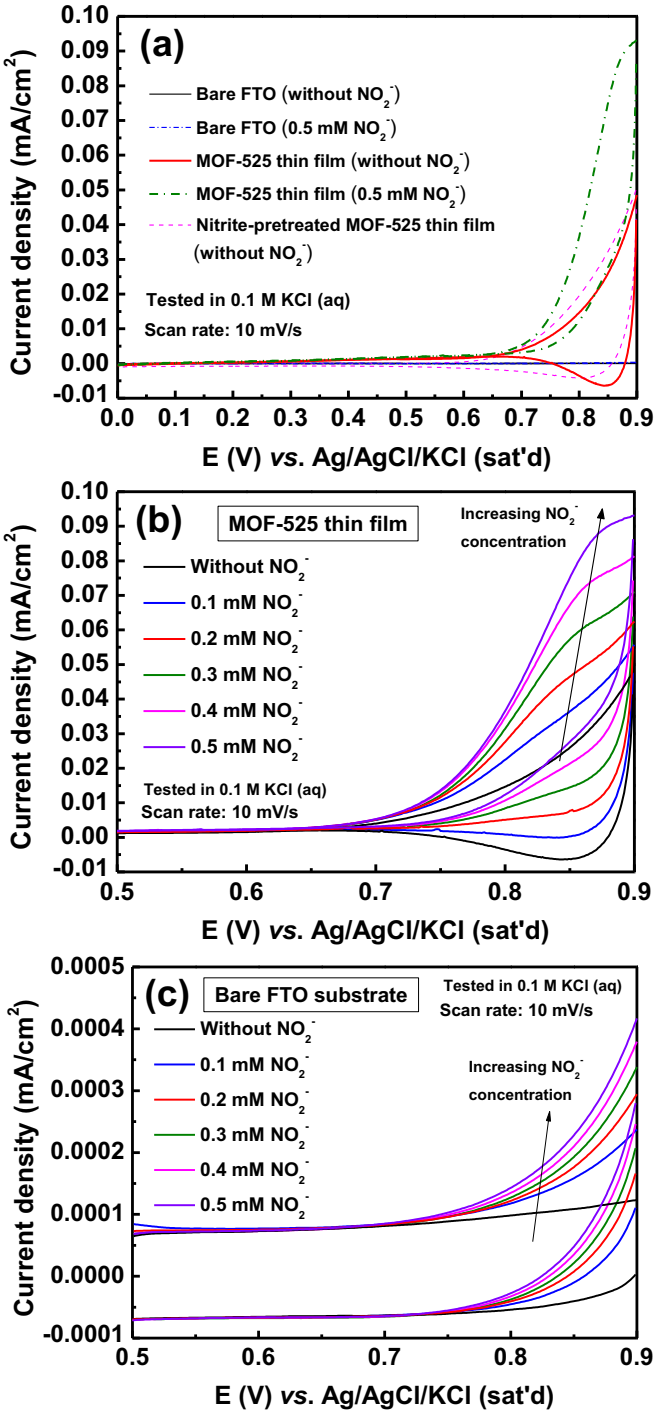

Fig. 2. (a) CV curves of the MOF-525 thin film and bare FTO substrate measured before and after adding 0.5 mM nitrite. CV curve of the pretreated MOF-525 thin film is also shown. (b) CV curves of the MOF-525 thin film and (c) bare FTO substrate, measured in various concentrations of nitrite.

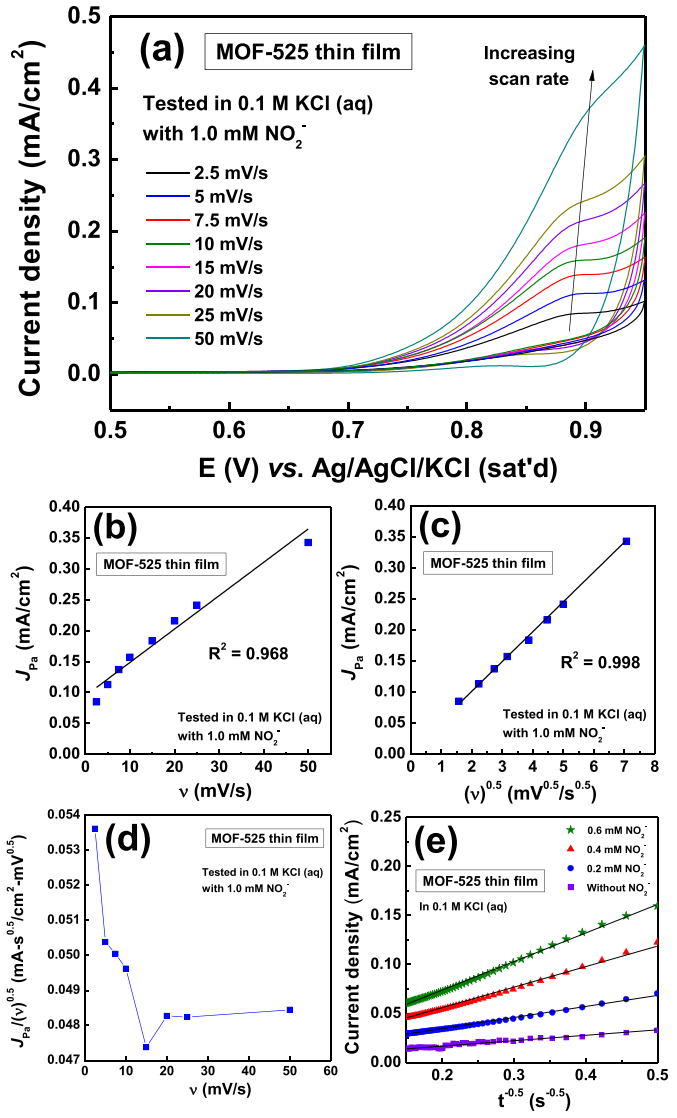

Fig. 3. (a) CV curves of the MOF-525 thin film measured in the solution containing 1.0 mM nitrite at various ν. Plots of (b) J_{pa} *vs.* ν, (c) J_{pa} *vs.* $\nu^{0.5}$, and (d) $J_{pa}/\nu^{0.5}$ *vs.* ν obtained from (a). (e) Plots of J *vs.* $t^{-0.5}$ obtained from the amperometric curves of the MOF-525 thin film measured at 0.9 V.

hopping between TCPP linkers need only take place in a part of the MOF thin film close to the underlying electrode. Thus, the values of D_{app} would increase after adding a small concentration of nitrite, since the diffusion rate of nitrite through the MOF-525 thin film is somewhat higher than the rate of linker-to-linker charge hopping in the thin film.

3.3. Amperometric detection of nitrite

An amperometric technique was used to quantify the concentration of nitrite by using the MOF-525 thin film. The amperometric curves of the MOF-525 thin film measured at 0.9 V in stationary 0.1 M KCl solutions containing various concentrations of nitrite are shown in Fig. 4(a), and the plot of current density recorded at 60 s *versus* the concentration of nitrite is shown in Fig. 4(b). Error bars were constructed from three separated experiments. From Fig. 4(b), it can be observed that the current density increases linearly with the increasing concentration of nitrite from 20 to 800 μM ($R^2 = 0.998$). From the slope of the calibration curve within this linear region, the sensitivity of the nitrite sensor can be estimated to be 95 μA/mM-cm^2. The limit of detection (LOD) of the proposed sensor is calculated to be 2.1 μM, based on the value of the sensitivity and a signal-to-noise ratio of 3. Compared to the sensitivities of electrochemical nitrite sensors reported recently [13,52–60], the sensitivity of the MOF-525 nitrite sensor is not superior, but it is still higher than some of them [52,53,56,59]. Moreover, the MOF-525 nitrite sensor exhibits a wider linear range compared to most of the sensors mentioned above [13,52,54,55,57,60]. The LOD reported here is smaller than that reported in one of the above studies [52]. Ongoing work is focusing on developing porphyrin MOF-based materials possessing faster charge-transport rates in order to improve the sensitivity and LOD.

4. Conclusions

Thin films of a MOF constructed from free-base porphyrin linkers and hexa-zirconium nodes (MOF-525) were grown on conducting glass substrates by using a solvothermal approach. The obtained MOF-525 thin film is electroactive in 0.1 M KCl aqueous solution, and it exhibits electrocatalytic activity for the oxidation of nitrite. The electrocatalytic process was found to be diffusion-controlled, and it was confirmed to be an ECcat process. The amperometric nitrite sensor using MOF-525 thin film was successfully developed.

Acknowledgments

This work was sponsored by the Ministry of Science and Technology (MOST) of Taiwan, under project NSC-103-2923-E-002-008-MY3. Work at Northwestern was supported by the U. S. Department of

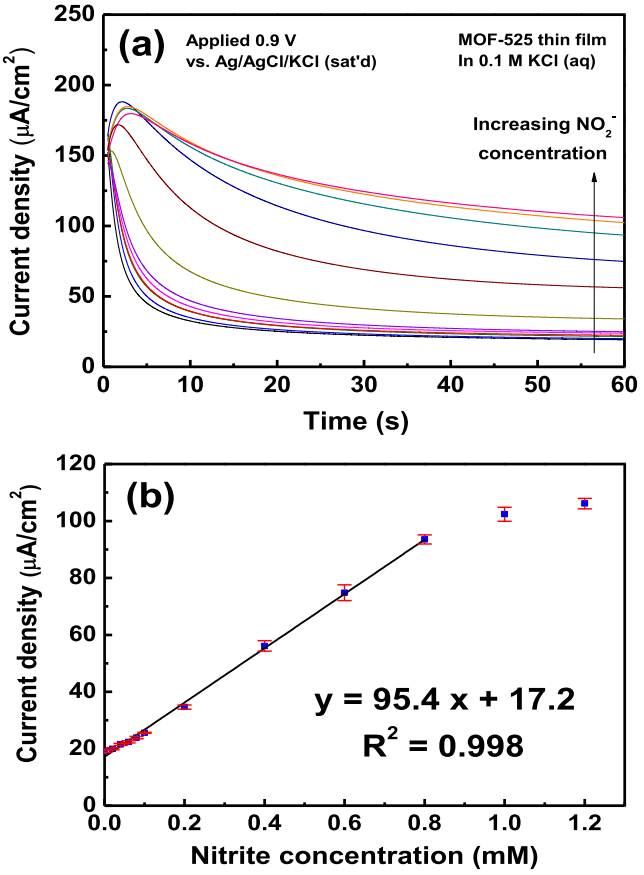

Fig. 4. (a) Amperometric curves of the MOF-525 thin film measured in the stationary solutions containing various concentrations of nitrite. (b) Plot of current density *vs.* concentration of nitrite.

Energy, Office of Science, Office of Basic Energy Sciences, under grant no. DE-FG87ER13808, and by Northwestern University.

References

[1] W. Lijinsky, S.S. Epstein, Nitrosamines as environmental carcinogens, Nature 225 (1970) 21–23.
[2] E. Morcos, N.P. Wiklund, Nitrite and nitrate measurement in human urine by capillary electrophoresis, Electrophoresis 22 (2001) 2763–2768.
[3] G. Ellis, I. Adatia, M. Yazdanpanah, S.K. Makela, Nitrite and nitrate analyses: a clinical biochemistry perspective, Clin. Biochem. 31 (1998) 195–220.
[4] É. Szökö, T. Tábi, A.S. Halász, M. Pálfi, K. Magyar, High sensitivity analysis of nitrite and nitrate in biological samples by capillary zone electrophoresis with transient isotachophoretic sample stacking, J. Chromatogr. A 1051 (2004) 177–183.
[5] I.M.P.L.V.O. Ferreira, S. Silva, Quantification of residual nitrite and nitrate in ham by reverse-phase high performance liquid chromatography/diode array detector, Talanta 74 (2008) 1598–1602.
[6] M. Bru, M.I. Burguete, F. Galindo, S.V. Luis, M.J. Marín, L. Vigara, Cross-linked poly(2-hydroxyethylmethacrylate) films doped with 1,2-diaminoanthraquinone (DAQ) as efficient materials for the colorimetric sensing of nitric oxide and nitrite anion, Tetrahedron Lett. 47 (2006) 1787–1791.
[7] P. Mikuška, Z. Večeřa, Simultaneous determination of nitrite and nitrate in water by chemiluminescent flow-injection analysis, Anal. Chim. Acta 495 (2003) 225–232.
[8] G. Wu, M.H. Zaman, Amperometric measurements of ethanol on paper with a glucometer, Talanta 134 (2015) 194–199.
[9] Y. Li, Y. Zhou, H. Xian, L. Wang, J. Huo, Electrochemical determination of nitrite and iodate based on Pt nanoparticles self-assembled on a chitosan modified glassy carbon electrode, Anal. Sci. 27 (2011) 1223–1228.
[10] A. Afkhami, F. Soltani-Felehgari, T. Madrakian, H. Ghaedi, Surface decoration of multi-walled carbon nanotubes modified carbon paste electrode with gold nanoparticles for electro-oxidation and sensitive determination of nitrite, Biosens. Bioelectron. 51 (2014) 379–385.
[11] H. Teymourian, A. Salimi, S. Khezrian, Fe_3O_4 magnetic nanoparticles/reduced graphene oxide nanosheets as a novel electrochemical and bioeletrochemical sensing platform, Biosens. Bioelectron. 49 (2013) 1–8.
[12] S. Liu, J. Tian, L. Wang, Y. Luo, X. Sun, Production of stable aqueous dispersion of poly(3,4-ethylenedioxythiophene) nanorods using graphene oxide as a stabilizing agent and their application for nitrite detection, Analyst 136 (2011) 4898–4902.
[13] H. Mao, X.C. Liu, D.M. Chao, L.L. Cui, Y.X. Li, W.J. Zhang, C. Wang, Preparation of unique PEDOT nanorods with a couple of cuspate tips by reverse interfacial polymerization and their electrocatalytic application to detect nitrite, J. Mater. Chem. 20 (2010) 10277–10284.
[14] Y.H. Cheng, C.W. Kung, L.Y. Chou, R. Vittal, K.C. Ho, Poly(3, 4-ethylenedioxythiophene) (PEDOT) hollow microflowers and their application for nitrite sensing, Sens. Actuators, B 192 (2014) 762–768.
[15] H. Winnischofer, S.D.S. Lima, K. Araki, H.E. Toma, Electrocatalytic activity of a new nanostructured polymeric tetraruthenated porphyrin film for nitrite detection, Anal. Chim. Acta 480 (2003) 97–107.
[16] C.M.N. Azevedo, K. Araki, L. Angnes, H.E. Toma, Electrostatically assembled films for improving the properties of tetraruthenated porphyrin modified electrodes, Electroanalysis 10 (1998) 467–471.
[17] C. Wang, R. Yuan, Y. Chai, S. Chen, Y. Zhang, F. Hu, M. Zhang, Non-covalent iron(III)-porphyrin functionalized multi-walled carbon nanotubes for the simultaneous determination of ascorbic acid, dopamine, uric acid and nitrite, Electrochim. Acta 62 (2012) 109–115.
[18] H. Furukawa, K.E. Cordova, M. O'Keeffe, O.M. Yaghi, The chemistry and applications of metal–organic frameworks, Science 341 (2013) 974.
[19] G. Férey, Hybrid porous solids: past, present, future, Chem. Soc. Rev. 37 (2008) 191–214.
[20] M.P. Suh, H.J. Park, T.K. Prasad, D.W. Lim, Hydrogen storage in metal–organic frameworks, Chem. Rev. 112 (2012) 782–835.
[21] J.R. Li, J. Sculley, H.C. Zhou, Metal–organic frameworks for separations, Chem. Rev. 112 (2012) 869–932.
[22] L.E. Kreno, K. Leong, O.K. Farha, M. Allendorf, R.P. Van Duyne, J.T. Hupp, Metal–organic framework materials as chemical sensors, Chem. Rev. 112 (2012) 1105–1125.
[23] L.Q. Ma, J.M. Falkowski, C. Abney, W.B. Lin, A series of isoreticular chiral metal–organic frameworks as a tunable platform for asymmetric catalysis, Nat. Chem. 2 (2010) 838–846.
[24] K.M. Choi, H.M. Jeong, J.H. Park, Y.B. Zhang, J.K. Kang, O.M. Yaghi, Supercapacitors of nanocrystalline metal–organic frameworks, ACS Nano 8 (2014) 7451–7457.
[25] G. Férey, F. Millange, M. Morcrette, C. Serre, M.L. Doublet, J.M. Greneche, J.M. Tarascon, Mixed-valence Li/Fe-based metal–organic frameworks with both reversible redox and sorption properties, Angew. Chem. Int. Ed. 46 (2007) 3259–3263.
[26] C.R. Wade, M.Y. Li, M. Dincă, Facile deposition of multicolored electrochromic metal–organic framework thin films, Angew. Chem. Int. Ed. 52 (2013) 13377–13381.
[27] C.W. Kung, T.C. Wang, J.E. Mondloch, D. Fairen-Jimenez, D.M. Gardner, W. Bury, J.M. Klingsporn, J.C. Barnes, R. Van Duyne, J.F. Stoddart, M.R. Wasielewski, O.K. Farha, J.T. Hupp, Metal–organic framework thin films composed of free-standing acicular nanorods exhibiting reversible electrochromism, Chem. Mater. 25 (2013) 5012–5017.
[28] O.K. Farha, I. Eryazici, N.C. Jeong, B.G. Hauser, C.E. Wilmer, A.A. Sarjeant, R.Q. Snurr, S.T. Nguyen, A.Ö. Yazaydın, J.T. Hupp, Metal–organic framework materials with ultrahigh surface areas: is the sky the limit? J. Am. Chem. Soc. 134 (2012) 15016–15021.
[29] C.Y. Zhang, M.Y. Wang, L. Liu, X.J. Yang, X.Y. Xu, Electrochemical investigation of a new Cu-MOF and its electrocatalytic activity towards H_2O_2 oxidation in alkaline solution, Electrochem. Commun. 33 (2013) 131–134.
[30] Y. Zhang, X. Bo, C. Luhana, H. Wang, M. Li, L. Guo, Facile synthesis of a Cu-based MOF confined in macroporous carbon hybrid material with enhanced electrocatalytic ability, Chem. Commun. 49 (2013) 6885–6887.
[31] B.Q. Yuan, R.C. Zhang, X.X. Jiao, J. Li, H.Z. Shi, D.J. Zhang, Amperometric determination of reduced glutathione with a new Co-based metal–organic coordination polymer modified electrode, Electrochem. Commun. 40 (2014) 92–95.
[32] B.Q. Yuan, J.C. Zhang, R.C. Zhang, H.Z. Shi, X.L. Guo, Y.Y. Guo, X.Y. Guo, S.S. Cai, D.J. Zhang, Electrochemical and electrocatalytic properties of a stable Cu-based metal–organic framework, Int. J. Electrochem. Sci. 10 (2015) 4899–4910.
[33] O.K. Farha, A.M. Shultz, A.A. Sarjeant, S.T. Nguyen, J.T. Hupp, Active-site-accessible, porphyrinic metal–organic framework materials, J. Am. Chem. Soc. 133 (2011) 5652–5655.
[34] D.W. Feng, Z.Y. Gu, J.R. Li, H.L. Jiang, Z.W. Wei, H.C. Zhou, Zirconium-metalloporphyrin PCN-222: mesoporous metal–organic frameworks with ultrahigh stability as biomimetic catalysts, Angew. Chem. Int. Ed. 51 (2012) 10307–10310.
[35] W. Morris, B. Volosskiy, S. Demir, F. Gandara, P.L. McGrier, H. Furukawa, D. Cascio, J.F. Stoddart, O.M. Yaghi, Synthesis, structure, and metalation of two new highly porous zirconium metal–organic frameworks, Inorg. Chem. 51 (2012) 6443–6445.
[36] R. Makiura, S. Motoyama, Y. Umemura, H. Yamanaka, O. Sakata, H. Kitagawa, Surface nano-architecture of a metal–organic framework, Nat. Mater. 9 (2010) 565–571.
[37] M.C. So, S. Jin, H.J. Son, G.P. Wiederrecht, O.K. Farha, J.T. Hupp, Layer-by-layer fabrication of oriented porous thin films based on porphyrin-containing metal–organic frameworks, J. Am. Chem. Soc. 135 (2013) 15698–15701.
[38] S.R. Ahrenholtz, C.C. Epley, A.J. Morris, Solvothermal preparation of an electrocatalytic metalloporphyrin MOF thin film and its redox hopping charge-transfer mechanism, J. Am. Chem. Soc. 136 (2014) 2464–2472.
[39] M.C. So, M.H. Beyzavi, R. Sawhney, O. Shekhah, M. Eddaoudi, S.S. Al-Juaid, J.T. Hupp, O.K. Farha, Post-assembly transformations of porphyrin-containing metal–organic framework (MOF) films fabricated *via* automated layer-by-layer coordination, Chem. Commun. 51 (2015) 85–88.
[40] C.W. Kung, T.H. Chang, L.Y. Chou, J.T. Hupp, O.K. Farha, K.C. Ho, Post metalation of solvothermally grown electroactive porphyrin metal–organic framework thin films, Chem. Commun. 51 (2015) 2414–2417.
[41] J.E. Mondloch, M.J. Katz, N. Planas, D. Semrouni, L. Gagliardi, J.T. Hupp, O.K. Farha, Are Zr_6-based MOFs water stable? Linker hydrolysis *vs.* capillary-force-driven channel collapse, Chem. Commun. 50 (2014) 8944–8946.
[42] Y.J. Tu, H.C. Cheng, I. Chao, C.R. Cho, R.J. Cheng, Y.O. Su, Intriguing electrochemical behavior of free base porphyrins: effect of porphyrin-meso-phenyl interaction controlled by position of substituents on meso-phenyls, J. Phys. Chem. A 116 (2012) 1632–1637.
[43] R. Guidelli, F. Pergola, G. Raspi, Voltammetric behavior of nitrite ion on platinum in neutral and weakly acidic media, Anal. Chem. 44 (1972) 745–755.
[44] B.R. Kozub, N.V. Rees, R.G. Compton, Electrochemical determination of nitrite at a bare glassy carbon electrode; why chemically modify electrodes? Sens. Actuators, B 143 (2010) 539–546.
[45] Y. Wang, E. Laborda, R.G. Compton, Electrochemical oxidation of nitrite: kinetic, mechanistic and analytical study by square wave voltammetry, J. Electroanal. Chem. 670 (2012) 56–61.
[46] A.J. Bard, L.R. Faulkner, Electrochemical Methods, Fundamentals and Applications, second edition John Wiley & Sons, New York, 2001.
[47] I. Gualandi, E. Scavetta, S. Zappoli, D. Tonelli, Electrocatalytic oxidation of salicylic acid by a cobalt hydrotalcite-like compound modified Pt electrode, Biosens. Bioelectron. 26 (2011) 3200–3206.
[48] C.W. Kung, Y.H. Cheng, K.C. Ho, Single layer of nickel hydroxide nanoparticles covered on a porous Ni foam and its application for highly sensitive non-enzymatic glucose sensor, Sens. Actuators, B 204 (2014) 159–166.
[49] C. Montella, Discussion of the potential step method for the determination of the diffusion coefficients of guest species in host materials: Part I. Influence of charge transfer kinetics and ohmic potential drop, J. Electroanal. Chem. 518 (2002) 61–83.
[50] M. Yagi, T. Sato, Temperature-controlled charge transfer mechanism in a polymer film incorporating a redox molecule as studied by potential-step chronocouloabsorptometry, J. Phys. Chem. B 107 (2003) 4975–4981.
[51] P. Bertoncello, I. Ciani, F. Li, P.R. Unwin, Measurement of apparent diffusion coefficients within ultrathin nafion Langmuir–Schaefer films: comparison of a novel scanning electrochemical microscopy approach with cyclic voltammetry, Langmuir 22 (2006) 10380–10388.
[52] M.R. Majidi, A. Saadatirad, E. Alipour, Pencil lead electrode modified with hemoglobin film as a novel biosensor for nitrite determination, Electroanalysis 25 (2013) 1742–1750.
[53] C. Qin, W. Wang, C. Chen, L. Bu, T. Wang, X. Su, Q. Xie, S. Yao, Amperometric sensing of nitrite based on electroactive ferricyanide–poly(diallyldimethylammonium)–alginate composite film, Sens. Actuators, B 181 (2013) 375–381.
[54] P. Li, Y. Ding, A. Wang, L. Zhou, S. Wei, Y. Zhou, Y. Tang, Y. Chen, C. Cai, T. Lu, Self-assembly of tetrakis(3-trifluoromethylphenoxy) phthalocyaninato cobalt(II) on multiwalled carbon nanotubes and their amperometric sensing application for nitrite, ACS Appl. Mater. Interfaces 5 (2013) 2255–2260.

[55] K. Dağcı, M. Alanyalıoğlu, Electrochemical preparation of polymeric films of pyronin Y and its electrolcatalytic properties for amperometric detection of nitrite, J. Electroanal. Chem. 711 (2013) 17–24.
[56] P. Muthukumar, S.A. John, Gold nanoparticles decorated on cobalt porphyrin-modified glassy carbon electrode for the sensitive determination of nitrite ion, J. Colloid Interface Sci. 421 (2014) 78–84.
[57] C. Wang, X. Zou, Q. Wang, K. Shi, J. Tan, X. Zhao, Y. Chai, R. Yuan, A nitrite and hydrogen peroxide sensor based on Hb adsorbed on Au nanorods and graphene oxide coated by polydopamine, Anal. Methods 6 (2014) 758–765.
[58] J. Jiang, W. Fan, X. Du, Nitrite electrochemical biosensing based on coupled graphene and gold nanoparticles, Biosens. Bioelectron. 51 (2014) 343–348.
[59] J. Wang, H. Zhou, D. Fan, D. Zhao, C. Xu, A glassy carbon electrode modified with nanoporous PdFe alloy for highly sensitive continuous determination of nitrite, Microchim. Acta 182 (2015) 1055–1061.
[60] S. Jiao, J. Jin, L. Wang, One-pot preparation of Au-RGO/PDDA nanocomposites and their application for nitrite sensing, Sens. Actuators, B 208 (2015) 36–42.